

Fisher Pruning of Deep Nets for Facial Trait Classification

Qing Tian, Tal Arbel, James J. Clark

Centre for Intelligent Machines & ECE Department, McGill University
3480 University Street, Montreal, QC H3A 0E9, Canada

Abstract. Although deep nets have resulted in high accuracies for various visual tasks, their computational and space requirements are prohibitively high for inclusion on devices without high-end GPUs. In this paper, we introduce a neuron/filter level pruning framework based on Fisher’s LDA which leads to high accuracies for a wide array of facial trait classification tasks, while significantly reducing space/computational complexities. The approach is general and can be applied to convolutional, fully-connected, and module-based deep structures, in all cases leveraging the high decorrelation of neuron activations found in the pre-decision layer and cross-layer deconv dependency. Experimental results on binary and multi-category facial traits from the LFWA and Adience datasets illustrate the framework’s comparable/better performance to state-of-the-art pruning approaches and compact structures (e.g. SqueezeNet, MobileNet). Ours successfully maintains comparable accuracies even after discarding most parameters (98%-99% for VGG-16, 82% for GoogLeNet) and with significant FLOP reductions (83% for VGG-16, 64% for GoogLeNet).

Keywords: deep nets pruning; facial trait classification; Fisher LDA

1 Introduction

Despite deep learning’s revolutionary success in many areas of computer vision, its high data and computational demands often make training from scratch impractical. As a result, the current popular practice is to adopt a general deep network model that has been pre-trained on a large, general dataset (e.g. ImageNet [1]) and fine-tune it for a specific inference task (e.g. facial trait recognition), usually based on a small dataset. However, in most cases, there is no theoretical justification for the ‘inherited’ structure. Some structures adapted from the pre-trained model can be sub-optimal or even dead (i.e. no activation) for the task in question. Parameters that are not well adapted to the task not only add to the storage and computational burden but also can result in overfitting [2] when the amount of data for fine tuning is small. In this paper, we explore the premise that less useful and/or redundant structures can be pruned away to boost both efficiency and accuracy.

The success of deep networks in visual classification tasks, including facial trait recognition, is largely attributed to its compositionality. Moving up the layers, complicated and more abstract high-level patterns can be built from simpler low-level patterns. One critical building block in this process is the filter/neuron, which, through

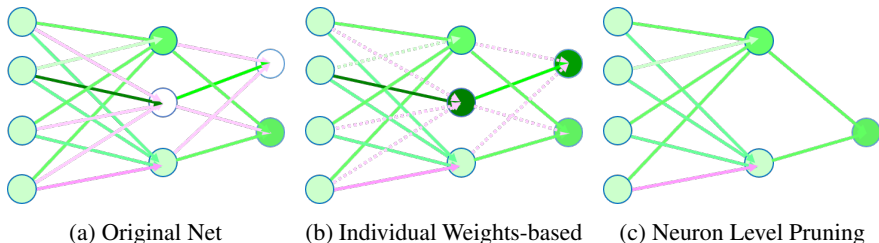


Fig. 1: Comparison of (b) individual weights based pruning [3] and (c) neuron level pruning on the example net in (a). Green: positive, magenta: negative, the darker the color, the larger the magnitude. Although the 2nd neuron in the hidden layer has a large positive input, its influence is counteracted by the joint force of the three small negative values. It follows that the neuron is not activated after ReLU. In (b), the second initially dormant neuron ends up firing strongly while (c) preserves the original firing patterns and thus the following output. The neuron level pruning in (c) illustrates the removal of dead neurons (it can perform more complex tasks). The pruned weights in (b) are represented by dashed lines as the resulting sparsity (in param matrices) is unstructured.

learning, is capable of capturing patterns or structures at a specific scale of abstraction. However, many current pruning approaches, such as [3], discard small but still ‘important’ filter/neuron weights individually, thus destroying the higher level pattern. Given the multiplication-accumulation-ReLU filter/neuron model and a uniform positive input, many small negative weights may join forces to counteract the influence of large positive weights and result in a dormant neuron. If pruning is based on individual weights, these small negative weights would be pruned before reaching the large positive weights. This results in serious problems (Figure 1). Such problems are more obvious when the pruning rate is high. In addition, we argue that pruning should also be task and data dependent.

In this paper, instead of treating weights individually, we develop a holistic dependency aware, neuron/filter level pruning framework based on Fisher’s LDA [4] on the last hidden layer neurons, which leads to significant space and computational savings with the possibility of boosting accuracy. This paper makes several critical improvements to previous work on filter level pruning [5]. To begin with, we extend the LDA pruning idea for convolutional layers (conv layers) to fully connected (FC) structures (either standalone FC nets or FC layers in a ConvNet), which makes LDA utility measure more accurate. In the ConvNet case, it means that the final pruning step is extended from the last conv layer (filters) all the way to the last hidden layer (neurons) of the whole net (in this paper, the last hidden layer is also called pre-decision layer which is immediately before the decision is made, softmax not included). This is important because FC layers usually dominate the model size (e.g. over 90% for both AlexNet [6] and VGG nets [7]) and we can now prune the full net in an end-to-end manner. Also, aside from conventional ConvNets (e.g. VGG-16), the method can be deployed on module-based structures (e.g. GoogLeNet [8] composed of Inception modules). We compare the pruning effectiveness of our approach to state-of-the-

art compact networks (e.g. SqueezeNet [9], MobileNet [10]) and two modern pruning approaches ([3,11]). More importantly, we discuss our pruning method’s general potential as a deep net structure design approach. Contemporary ‘skinny’ nets such as SqueezeNet, MobileNet, and GoogLeNet leverage many $1*1$ filters (at the module beginning/end). From our perspective, those filters serve to reduce dimensionality in an ad-hoc manner. What’s worse, for popular deep modules such as Inception modules and Fire modules (in SqueezeNet), the filter number for each filter size is set arbitrarily. Although those nets perform well for a particular task, their generalizability/adaptability may be compromised. By handling module based structures, our task-specific approach offers a solution to these challenges. From a dimensionality reduction perspective, our approach is able to determine the type of filters required as well as the number required. For example, in the age group classification experiments on Adience [12] using GoogLeNet, $1*1$ and $5*5$ scale filters in the Inception_5b module contain little information, while they are indispensable in Inception_5a. In general, $3*3$ filters are of greater importance than others across layers. The approach presented here is to boost efficiency while reducing over-fitting. As was found in previous work [5] in the context of gender recognition using VGG-16, conv filter firings tend to be progressively more decorrelated when navigating from the bottom to the top conv layer of a deep convolutional net. Through Fisher’s LDA, it is possible to discard conv5_3 filters directly. In this paper, we extend and further elaborate on this and formulate it as solving a generalized eigenvalue problem. In our experiments of recognizing facial traits (i.e. gender, smile, and age as person specific/non-specific, binary/multi-category examples), we show how the proposed method leads to significant complexity reductions: bringing down the total VGG-16 size by 98%-99% and that of GoogLeNet by 82% without significant accuracy loss ($<1\%$). The corresponding FLOP reduction rates are about 83% and 62%, respectively.

2 Related Work

2.1 Facial Trait Classification

Facial trait or attribute classification has received wide attention over the years. Traditional approaches use global [13,14] and/or local [15,16,17,18,19] hand-crafted features plus classic machine learning classification techniques such as SVM and Bayesian QDA (alone or with some boosting algorithm). However, this process is hand-engineered subjectively and may not generalize well. With the popularity of deep learning, the ‘features and classifiers’ are learned by artificial neural nets in an end-to-end manner, which have generally led to better performance given enough data. In the 1990s, early neural networks began to be employed for facial trait classification [20,21,22]. However, the shallow structures constrained their performance and applicability. Since the overwhelming success of AlexNet [6] in the 2012 ImageNet Challenge, a variety of deep nets have been successfully applied to a multitude of visual recognition tasks including facial trait classification. Verma *et al.* [23] showed the similarities between the CNN filters learned and the features that neuroscientists identified as cues utilized by humans to recognize facial attributes such as gender. Inspired by the dropout technique in deep nets training, Eidinger *et al.* [12] trained an SVM with random dropout of some features and

achieved promising results on their Adience dataset. Levi and Hassner [24] later trained and tested a not-very-deep CNN for gender and age recognition on the same dataset, but with better performance. Rather than train on images of full faces, Mansanet *et al.* [25] employed local patches to train relatively shallow nets and obtained better accuracies than full face image-based nets of similar depths. To make better use of shape information, Li *et al.* [26] proposed shape adaptive kernel-based tree-structured CNNs for facial trait classification. Through pose-normalized CNNs, Zhang *et al.* [27] combined part-based models with deep nets. Liu *et al.* [28] leveraged two CNNs to detect face regions and recognize facial traits sequentially, and reported state-of-the-art accuracies on the LFWA dataset. Given enough training data and reasonable building block modules, larger depths generally lead to higher accuracies [7,29]. However, compared to datasets for face recognition/verification, large datasets with facial trait labels are relatively rare. Therefore, facial trait classification is often based on identity features learned for recognition/verification tasks (e.g. [30]), even though these features may not be optimal for the task. Finally, to recognize facial traits efficiently, we argue that it is desirable to directly disentangle useful structures from possibly redundant and less useful ones.

2.2 Deep Neural Networks Pruning

Early approaches to artificial neural networks pruning date back to the late 1980s. Some pioneering examples include magnitude-based biased weight decay [31], Hessian based Optimal Brain Damage [2] and Optimal Brain Surgeon [32]. Since those approaches were aimed at shallow nets, assumptions that were made, such as a diagonal Hessian in [2], are not necessarily valid for deep neural networks. We refer our readers to [33] for more examples of early work in this area. The focus of the remainder of this section is on those approaches designed for deep nets.

Over the past few years, popular deep nets have become deeper and deeper. However, with larger depths comes more complexity. This re-ignited research into network pruning. Han *et al.* [3] locate important network connections by finding weights that have large magnitudes after training. In [34], they added two more stages of weight quantization and Huffman encoding in order to further reduce the network complexity. Since their pruning is based on individual weights, it may not well reflect larger scale utilities (within layer/filter or across layers). In terms of implementation, small weights are set to zero and masks are needed to freeze/disregard those weights. Although, through compression, smaller models are possible for storage and transferring, the actual model size and computations remain the same after being deployed on general machines. Similar approaches [35,36,37,38,39,40] sparsify networks by setting weights to zero. Unlike the above approaches, Anwar *et al.* [41] locate pruning candidates via particle filtering in a structured way. Since candidate selection masks are generated randomly, they may miss crucial candidates' relationships.

Recently, conv filter pruning has gained more popularity [42,11,5]. From a practical perspective, they are appealing for the reason that they can directly produce hardware friendly architectures that not only reduce the requirements of storage space and transportation bandwidth, but also bring down the initially huge amount of computation in conv layers. Moreover, with fewer intermediate feature maps generated and consumed, the number of slow and energy-consuming memory accesses is also decreased. Besides

such utilitarian reasons, we can also draw inspiration for filter/neuron level pruning from findings in neuroscience [5]. According to [43], in spite of the huge number of neural connections in the brain, each neuron typically receives inputs from only a small set of others given a specific task. It has also been demonstrated both anatomically and functionally that mini-columns [44,45] in the cortex have accompanying functionalities that only become clear when seen on the higher macro-column level where the activations are sparse [46,47]. However, most previous filter-level pruning approaches could not accurately capture the utility for final classification. For example, Polyak and Wolf [42] proposed a ‘channel-level’ acceleration algorithm for deep face representations. However, the channel selection in their approach is local and is based on unit variances. Unwanted variances (e.g. lighting, pose, and makeup) and noise can be preserved or even amplified by their approach. Another approach, by Li *et al.* [11], equates filter utility to absolute weights sum. These filter-level pruning approaches were also not able to capture larger scale utility for final classification/recognition. It is also worth noting that aside from pruning, some approaches constrain space and computational complexity through reducing weight bitwidth (e.g. XNOR-Net and BWN [48]) at the expense of accuracy. Another way is to adopt compact layers/modules with fewer weights (e.g. NiN [49], GoogLeNet [8], ResNet [50], SqueezeNet [9], and MobileNet [10]).

3 LDA-based Neuron Level Pruning for Deep Nets

In this paper, we treat pruning as a dimensionality reduction problem in the (conv/FC) feature space. The goal is to disentangle the factors of variation and discard the ones that we are not interested in. From our perspective, previously mentioned compact nets such as SqueezeNet, MobileNet, and GoogLeNet are able to achieve significant compression/reduction rates mainly because of the $1*1$ filters utilized (usually at the module beginning), whose effects could be considered as reducing dimensionality (on the filter/neuron level). Unfortunately, these $1*1$ filters are selected in an relatively ad-hoc manner. In contrast, we develop a pruning framework based on Fisher’s LDA of the last hidden layer neuron activations (right before where the net branches into final decisions). Through deconvolution, this LDA-based final classification utility is traced backwards across all layers to weigh the usefulness of each neuron/filter and help decide which ones to abandon. In this way, our approach has derived optimal structures for a particular task with possible accuracy boosts. The holistic utility awareness also distinguishes ours from individual/local magnitudes/variances based approaches such as [3,11,42].

Unlike previous works with less accurate utility measures from conv layers [5,11], we argue that for a classification task (e.g. facial trait recognition), the utility measure should be the final discriminating power between the classes. Thus, we start pruning (or dimensionality reduction in our view) from the last hidden layer. It is of particular importance for LDA-based utility measures as data in the pre-decision layer is more likely to be linearly separable (an assumption of LDA). In this paper, targeted at the facial trait recognition problem, we use both conventional and module-based deep nets (i.e. VGG-16 [7] and GoogLeNet [8]) to illustrate the method.

3.1 Dimensionality Reduction in Last Hidden Layer

We begin by fully training a base deep net, using a cross entropy loss with L2 regularization and Dropout (that can help punish co-adaptations), before pruning it. Besides the reason that all previous neurons feed to the last hidden layer and only this layer's neurons directly contribute to the final discrimination, we prune from this layer because pre-decision neuron activations (duplicates removed) are shown empirically to fire in a more decorrelated manner than earlier layers. We will see how it helps our pruning.

We define the activation value of a neuron as its firing score. For filters with more than one weight, we take its maximum. Thus, for each sample image, an M -dimension firing vector can be calculated in the pre-decision layer, which we call a *firing instance* or observation ($M = 4096$ for VGG-16, $M = 1024$ for GoogLeNet). By stacking all these observations from a set of images, the firing data matrix X for that set is obtained (many 0 or duplicate columns are pre-removed). Unlike unsupervised dimensionality reduction techniques with general utility measures (e.g. high variance for PCA, the reconstruction potential for autoencoders), our aim here is to abandon dimensions in X with less discriminating power for final classification given the labels. Inspired by previous work [5,14,51,52], we adopt Fisher's LDA [4] to quantify the information utility for facial trait classification. The goal of Fisher LDA is to maximize the class separation by finding an optimal transformation matrix W :

$$W_{opt} = \arg \max_W \frac{|W^T \Sigma_b W|}{|W^T \Sigma_w W|} \quad (1)$$

where

$$\Sigma_w = \frac{1}{C} \sum_i \frac{1}{N_i - 1} \tilde{X}_i^T \tilde{X}_i \quad (2)$$

$$\Sigma_b = \Sigma_a - \Sigma_w \quad (3)$$

$$\Sigma_a = \frac{1}{N - 1} \tilde{X}^T \tilde{X} \quad (4)$$

with X_i being the set of observations obtained in the last hidden layer for category i (i is 0/1 for binary traits). N_i indicates the number of observations in category i and N is the number of total observations. W projects the data X from its original space to a new space spanned by its columns. The tilde sign ($\tilde{\cdot}$) denotes a centering operation; for data X this means:

$$\tilde{X} = (I_n - n^{-1} \mathbf{1}_n \mathbf{1}_n^T) X \quad (5)$$

where n is the number of observations in X , $\mathbf{1}_n$ denotes an $n \times 1$ vector of ones. Finding W_{opt} involves solving a generalized eigenvalue problem, which can be formulated as:

$$\Sigma_b e_j = v_j \Sigma_w e_j \quad (6)$$

where e_j represents a generalized eigenvector of the transformation matrix W with v_j as the corresponding generalized eigenvalue ($j < M - 1$). In our experiments, we find that most off-diagonal values in Σ_w and Σ_b are very small, which is to say, the

firings of different neurons in the pre-decision layer are highly uncorrelated (within or between the classes). This is due to the fact that coincidences/agreements in high dimensions can hardly happen by chance. It also corresponds to the intuition that, unlike common primitive features in lower layers, higher layers capture high-level abstractions of various aspects (e.g. car wheel, dog nose, flower pedals). The chances of them firing simultaneously are relatively low. Thus, it is a reasonable assumption that Σ_w and Σ_b are diagonal. Since dead (and duplicate) neurons are pre-removed, Equation 6 becomes:

$$(\Sigma w^{-1} \Sigma_b) e_j = v_j e_j \quad (7)$$

According to Equation 7, W columns (e_j , where $j = 0, 1, 2, \dots, M' - 1$, $M' < M$) are the eigenvectors of $\Sigma w^{-1} \Sigma_b$ (which is also diagonal), thus they form the standard basis vectors of the M' -dimension space (i.e. W columns and M' of the original neuron dimensions are aligned), and v_j are the corresponding eigenvalue with:

$$v_j = \text{diag}(\Sigma w^{-1} \Sigma_b)_j = \frac{\sigma_b^2(j)}{\sigma_w^2(j)} \quad (8)$$

where $\sigma_w^2(j)$ and $\sigma_b^2(j)$ are within-class and between-class variances along the j th neuron dimension. In other words, the optimal W columns that maximize the class separation (Eq. 1) are aligned with (a subset of) the original neuron dimensions. It turns out that when reducing dimensionality, we can directly discard dimension j s with small v_j (high within-class variances and low between-class variances) without much information loss. For example, in gender recognition, although both a mustache neuron and a glasses neuron have high variances that PCA prefers, the mustache neuron is selected by Fisher's LDA due to its large contribution to class separation (Eq. 1).

3.2 Deconv-based Utility Tracing for Cross-Layer Pruning

Dimensionality reduction based on useful neuron activations in the pre-decision layer makes structured pruning possible. A pruning unit based on filters/neurons focuses on the activation itself (nonlinear activation after weighted sum). The higher layers, which focus on the final discriminability, are agnostic as how they are activated, in terms of the weights and input details. Figure 2 is an overview of our LDA-based full-net neuron/filter level pruning approach. The useful (cyan) activations (e.g. neuron outputs/feature maps) that contribute to final classification through corresponding next layer weights/filter depths (green), only depend on previous layers' (cyan) counterparts.

We measure neuron/filter's utility by tracing the final discriminability backwards via deconvolution (deconv) [53,54], across all layers till the image space. As an inverse process of convolution (followed by nonlinear activation and pooling), deconv reconstructs the contributing sources of useful disentangled firing patterns. A unit deconv procedure is composed of unpooling (using stored max location switches), nonlinear rectification, and reversed convolution (a transpose of the convolution Toeplitz matrix under an orthonormal assumption). As the name indicates, deconv is originally designed for conv layer filters. In this paper, we extend the deconv idea to FC structures. This is partially inspired by [55,5]. However, unlike fully convolutional nets, we do not need to preserve

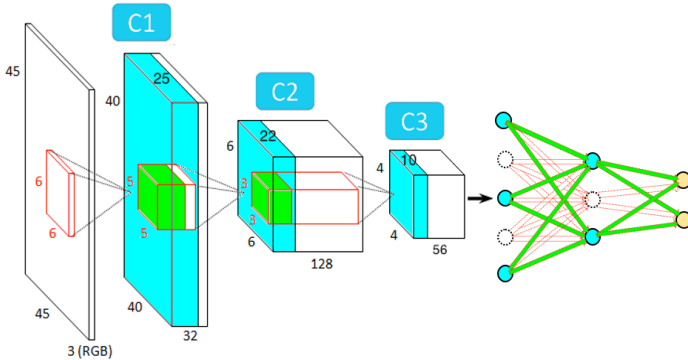


Fig. 2: Overview of our full-net neuron/filter level pruning. Cyan indicates feature maps (or neuron activations for FC layers) that have large influences on the final classification, green represents the corresponding parts of a next layer filter (or weights in FC layers). White denotes things (filter pieces, feature maps, neuron weights and outputs) that are less relevant to the final LDA utility in the pre-decision layer.

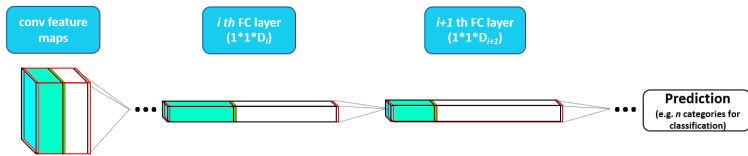


Fig. 3: Diagram depicting deconv-based dependency in FC layers where a layer’s input and weights are considered as a stack of $1*1$ conv feature maps and $1*1$ conv filters, respectively. The next layer’s filter and this layer’s data (feature maps) overlap completely; their size is specified in parentheses. For FC nets, there is no first column.

location information for FC structures. Our idea is illustrated in Figure 3. As opposed to normal conv layers, pure FC structures can be considered as special CNNs where each neuron is a stack of $1*1$ filters with one $1*1$ output feature map. Such structures do not have pooling layers in-between (or equivalently, the pooling kernel is of size $1*1$). As for a CNN-connected FC layer, it can also be treated as a special convolution layer where the 2D convolution kernel, pooling kernel and pooling stride are of the same size as one input feature map. Instead of selecting the max, the pooling layer selects the center value (a weighted average pooling operation with 0 weights everywhere off the center). Thus, for either pure FC structures or CNN-connected FC layers, 2D max switches are not necessary for unpooling. Re-structured in this way, the final (hidden layer) classification utility computed using LDA can be successfully passed back across all layers in a deep net. Our full net pruning, (re)training, and testing is not only more accurate but also more efficient given the wide availability of end-to-end deep learning libraries. This is different from the previous method [5] that chops off FC layers and replaces FC layers with light alternatives. It is worth mentioning that the dependency here is data-driven and is learned by pooling over the training set, which models the estab-

lished phenomenon in neuroscience which stipulates that multiple exposures are able to strengthen relevant connections (synapses) in the brain (the Hebbian theory [56]).

With all neurons/filters’ utility for final discriminability known, the pruning process involves discarding structures that are less useful to final classification (structures colored white in Figures 2 and 3). When all dependencies on a neuron/filter from above layers are discarded, this neuron/filter can be abandoned. Since feature maps (neuron outputs) correspond to next-layer filter depths (neuron weights), our LDA based neuron/filter level pruning leads to both filter-wise and channel-wise savings (FC structures are considered as special conv layers). Mathematically speaking, input of conv layer i can be defined as one data block $B_{data,i}$ of size $d_i \times m_i \times n_i$ meaning that the input is composed of d_i feature maps of size $m_i * n_i$ (from layer $i - 1$). Parameters of conv layer i can be considered as two blocks: the conv parameter block $B_{conv,i}$ of size $f_i \times c_i \times w_i \times h_i$ and the bias block $B_{bias,i}$ of size $f_i \times 1$, where f_i is the 3D filter number of layer i , c_i is the filter depth, w_i and h_i are the width and height of a 2D filter piece in that layer. It is worth noting that $f_{i-1} = d_i = c_i$. $B_{conv,i}(:, k, :, :)$ operates on $B_{data,i}(k, :, :)$, which is calculated using $B_{conv,i-1}(k, :, :, :)$ (‘:’ indicates all values along a certain dimension). When we prune away $B_{conv,i-1}(k, :, :, :)$, we effectively abandon the other two. In other words, $B_{conv,i}$ is pruned along both the first and second dimensions over the layers. During pruning, neurons with a LDA-deconv utility score smaller than a threshold are deleted. In practice, LDA-Deconv dependencies are sparse (i.e. useful neurons/filters are at high percentiles) in most layers of large nets. To get rid of massive useless neurons quickly while be cautious in high utility regions, we set the threshold for layer i as:

$$t_i = \eta \sqrt{\frac{1}{N-1} \sum_{j=1}^N (x_j - \bar{x}_i)^2} \quad (9)$$

where \bar{x}_i is the average utility (useful firing) score of all layer i neurons/filters, x_j is the utility score of the j th neuron/filter, and N is the total neuron/filter number in layer i . For it to work well, one assumption is that LDA-deconv utility scores in a certain layer follow a Gaussian-like distribution. Since η is constant over all layers, there is only one pruning time hyper-parameter η to set overall, which is directly related to the pruning rate. We can set it either to squeeze the net as much as possible without obvious accuracy loss or to find the ‘best’ structure with the highest accuracy, or to any possible pruning rate according to the resources available and accuracies expected. In other words, rather than a particular compact model (such as SqueezeNet or MobileNet), we offer the flexibility to create models customized to different needs. Also, our ‘model designer’ is advantageous over fixed compact nets in that the latter’s adaptability is sacrificed with greatly reduced capacity. Therefore, although they are able to achieve state-of-the-art performance on the task they are designed for, they may not perform well on new tasks or data. We will illustrate this through facial trait recognition in our experiments. Moreover, as mentioned previously, modern compact nets achieve significant compression rates mainly because of the use of 1*1 filters. However, unlike our LDA based pruning approach, the ad-hoc ‘dimensionality reduction’ using a random number of 1*1 filters has no theoretical justification. For our approach, one time retraining with the surviving parameters is needed after pruning.



Fig. 4: Images from the LFWA dataset (male/female, smiling/non-smiling examples).



(a) 0-2 (b) 4-6 (c) 8-13 (d) 15-20 (e) 25-32 (f) 38-43 (g) 48-53 (h) 60+

Fig. 5: The 8 age groups in the Adience dataset with one example for each group.

4 Experiments and Results

In this paper, we pre-train our models on the ImageNet dataset [57], then fine-tune and test them for facial trait classification on the LFWA [28] and Adience [12] datasets (i.e. gender, smile from LFWA, and age group from Adience). These traits are chosen as examples of binary/multi-class, person specific/non-specific facial attributes. The LFWA dataset is a richly labeled version of the Labeled Faces in the Wild (LFW) database [58] and has over 13K images with 40 facial trait labels. Another dataset used is the Adience dataset, which consists of 26K images of 2,284 subjects with age group and gender labels. Both datasets cover a large range of pose and background clutter variations. The suggested splits in [28,24] are adopted. For Adience, we use the first three folds for training, the 4th and 5th folds for validation and testing. All images are pre-resized to 224×224 . Figure 4 and 5 are examples from the two datasets for our interested traits.

4.1 Accuracy v.s. Number of Pre-decision Layer Neurons

We first demonstrate our utility measure’s effectiveness in selecting neurons in last hidden layer for classification. Figure 6 shows the relationship between recognition accuracy and the number of neurons preserved in the pre-decision layer. The top k neurons with highest Fisher’s LDA scores are used for the final prediction. As we can see, out of thousands of neurons in the last hidden layer (4096 for VGG-16, 1024 for GoogLeNet), only a few LDA-selected neurons can lead to a comparable accuracy with the original net. Thus, we plot only the cases of $k = 1, \dots, 100$. This intuitively demonstrates our neuron selection strategy’s effectiveness and experimentally confirms the hypothesis that a great deal of less useful (or duplicate) structures exist.

4.2 Accuracy v.s. Pruning Rates

In this section, we analyze accuracy change v.s. complexity reductions. Figure 7 demonstrates the relationship of accuracy change with the number of parameters pruned. For comparison purposes, we add to the figures the performance of two other pruning approaches (i.e. Han *et al.* [3] and Li *et al.* [11]) as well as modern compact/pruned structures such as SqueezeNet [9] and MobileNet [10]. According to Figure 7, even with a large percentage of the parameters having been pruned away (98-99% for the VGG-16

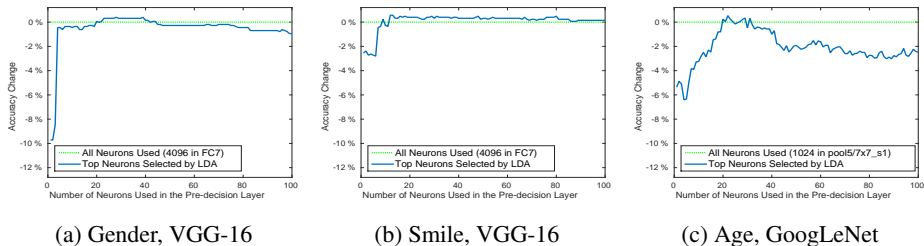


Fig. 6: Accuracy change vs. number of neurons selected by LDA in pre-decision layer.

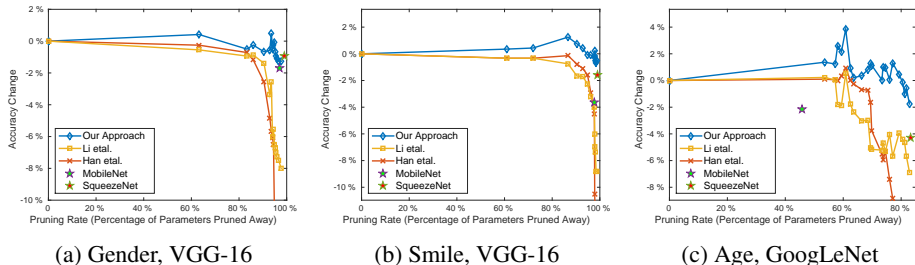


Fig. 7: Accuracy change vs. parameters savings of ours (blue), Han *et al.* [3] (red), and Li *et al.* [11] (orange). For comparison, the performance of SqueezeNet [9] and MobileNet [10] have been added. The ‘parameter pruning rate’ for them implies the relative size w.r.t the whole VGG-16 or GoogLeNet. In our implementation of [11], we adopt the same pruning rate as ours in each layer (rather than determine them empirically).

cases, 82% for the GoogLeNet case), our approach still maintains comparable accuracy to the original models, with a loss within 1%. The other two pruning approaches suffer from earlier performance degradation. This is primarily due to their utility measure. Additionally, for [3], inner filter relationships are vulnerable to pruning especially when the pruning rate is large. This also explains why Li *et al.* [11] beats Han *et al.* [3] at large pruning rates although the later approach has, generally speaking, slightly higher accuracies at early stages. It is worth noting that during the pruning process, we come across even more accurate but lighter structures than the original net. For instance, in the age case, a model of 1/3 the original size is 3.8% more accurate than the original GoogLeNet. Similarly in the smile trait case, a 5x times smaller model can achieve 1.5% more accuracy than the unpruned VGG-16 net. That is to say, in addition to boosting efficiency, our approach provides a way to find optimal deep models while being mindful of the resources available. Compared to the fixed compact nets (SqueezeNet and MobileNet), our pruning approach generally enjoys better performance because ‘dimensionality reduction’ in the feature space with a utility measure that is directly related to final classification is superior to reducing dimension using an arbitrary number of 1*1 filters. The performance differences also support our claim that pruning should be task specific. Even in the only pruning time exception, where our approach has a slightly lower accuracy at the same size of SqueezeNet, higher (than SqueezeNet) accuracies can be gained by simply adding back a few more parameters.

Since the previous approach [5] chops off size-dominant FC layers and only prunes the conv layers, it is not directly comparable with this paper’s approach in terms of parameters. Since conv layers account for most computation, we compare them in terms of accuracy vs. computation (FLOP¹) saved on the VGG-16 structure (Figure 8).

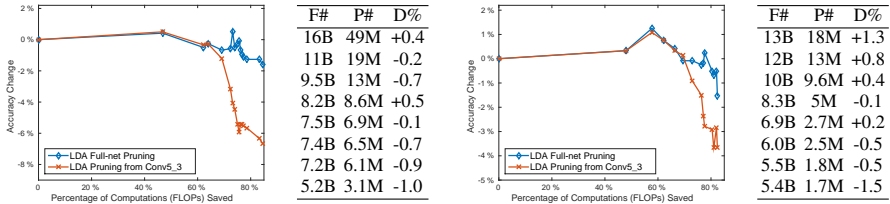


Fig. 8: Accuracy change vs. FLOP savings of this paper’s approach (blue) and [5] (red) for the gender (left) and smile (right) traits on VGG-16. In each figure’s accompanying table, F# and P# represent FLOPs and number of parameters, respectively. D% stands for accuracy difference with the original unpruned net. Both approaches share the same F#, while the P# and D% are of this paper’s approach. FC+Softmax is used for [5].

As can be seen, the two pruning approaches perform almost the same when the pruning rate is low. However, when the pruning rate increases, this paper’s full-net pruning approach enjoys higher accuracies than [5], which only prunes conv layers. The accuracy difference can be as large as 6% (on validation data). The reason is that our LDA-utility is calculated in the last hidden layer, which is more directly related to final classification power. Also, in that layer, data is more likely to be explained by linear combinations of variables (a key LDA assumption).

To assess generalization ability on unseen data, in Table 1, we select our model with the highest accuracy (accuracy first strategy) and the lightest one with less than 1% accuracy loss (param# first strategy) on the validation data for each task, and report

Table 1: Accuracy comparison on the testing data. ‘AF’ and ‘PF’ represents accuracy first and param# first strategies when selecting our models. Our approach’s param# and FLOPs (last row) are respectively shared by [11,3] and [11,5]. [3] has the same FLOPs as the base models. The base models’ testing accuracies are included in the first row parentheses. Original param# and FLOPs for VGG-16, GoogLeNet, MobileNet, and SqueezeNet are 138M, 6.0M, 4.3M, 1.3M and 31B, 3.2B, 1.1B, 1.7B, respectively.

Methods & Acc	Gender (VGG, 91%)		Smile (VGG, 91%)		Age (GoogLeNet, 55%)	
	AF	PF	AF	PF	AF	PF
MobileNet [10]	89%		87%		49%	
SqueezeNet [9]	89%		88%		50%	
Han <i>et al.</i> [3]	89%	83%	91%	81%	56%	43%
Li <i>et al.</i> [11]	88%	85%	91%	83%	56%	46%
Tian <i>et al.</i> [5]	90%	88%	92%	88%	58%	54%
Our approach	93%	92%	93%	90%	58%	54%
(Param#,FLOP)	(6.5M,7.4B)	(3.1M,5.2B)	(18M,13B)	(1.8M,5.5B)	(2.3M,1.8B)	(1.1M,1.1B)

¹ As in [3], both multiplication and addition account for one FLOP in this paper.

accuracies on the test sets. The competing approaches are added for comparison. From Table 1, it is evident that our approach generalizes well to unseen data (highest accuracies over most cases). Its superiority is more obvious in the ‘parameter# first’ case. This agrees with the previous validation results. Additionally, the accuracy margins between our pruning approach and the fixed nets are wider than on validation data partly because of fixed nets’ arbitrary and task independent way of ‘selecting’ filter dimensions. Finally, our approach performs better on the GoogLeNet than on the VGG-16s as the former gives ours the flexibility to select filter types/sizes in addition to filter numbers.

4.3 Layerwise Complexity Analysis

In this section, we provide a layer-by-layer complexity analysis of our pruned nets in terms of parameters and computation. The net we select for each case is the one that preserves similar classification power (loss within 1%) to the original net, but with as few parameters as possible. Figure 9, 10, 11 demonstrate layer-wise complexity reductions of the gender, smile/no smile, and age cases respectively. The base model for the former two is VGG-16, and the one in the age case is GoogLeNet. Since parameters in fully connected layers dominate the whole VGG-16 net, we add a separate layer-wise parameter analysis for conv layers in the two VGG-16 cases. From these results, it is

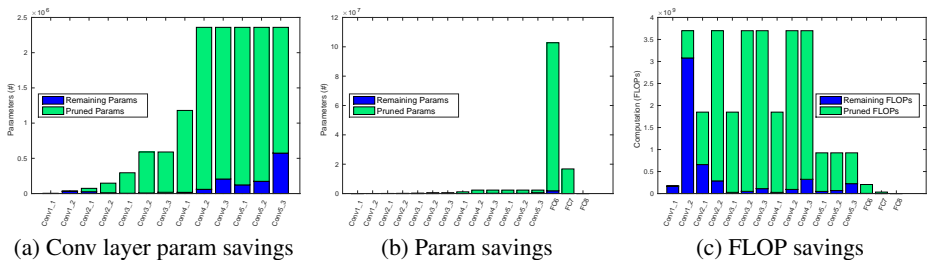


Fig. 9: Layerwise complexity reductions (gender, VGG16).

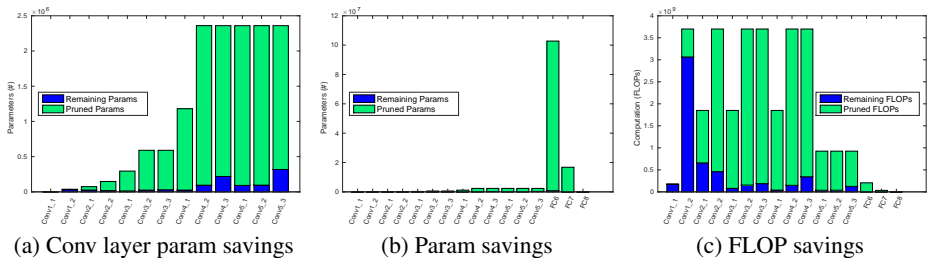


Fig. 10: Layerwise complexity reductions (smile, VGG16).

evident that our approach has led to significant parameter and FLOP reductions across layers. Particularly, the reduction in parameters for the VGG-16 models mainly come from the first FC layer (i.e. FC6) due to the fact that the last conv layer output (after pooling) still has so many ‘pixels’ that, when connected with all first FC layer’s neurons (4096 in VGG-16), they generate a huge number of parameters. Even though there are many conv filters, the total conv parameter number has nothing to do with input feature

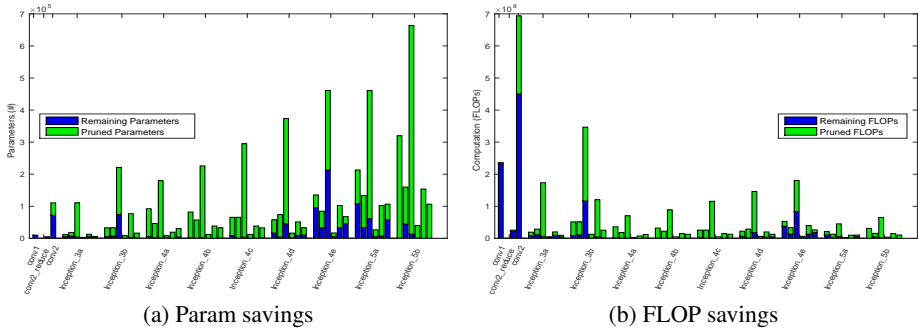


Fig. 11: Layerwise complexity reductions (age, GoogLeNet). From left to right, the conv layers in a Inception module are $(1*1)$, $(1*1, 3*3)$, $(1*1, 5*5)$, $(1*1$ after pooling).

map (2D) dimension thanks to the weight sharing scheme. We can also see that higher layers, in general, have higher parameter pruning rates than the first three layers. This makes sense as earlier layers correspond to primitive patterns (e.g. edges, corners, and color blobs) that are commonly useful. Figure 11 shows the case of classifying age with GoogLeNet as the base model. In each Inception model, different kind of filters are pruned differently. For example, from right, the 2nd-4th modules prefer $1*1$ and $5*5$ filters more than other modules do. $3*3$ filters are generally more desirable than others. In pruned Inception_5b, $3*3$ is the only filter type left. As we can see, our approach provides a way to design deep architecture by choosing the kinds of filters and also the filter number for each kind. One thing in common between our pruned VGG-16 and GoogLeNet models is that most parameters in the middle layers have been discarded. Those filters can possibly be collapsed to reduce net depth. For instance, most of the few filters left in the middle modules in Figure 11 are of size $1*1$. They can be viewed as filter selectors (by weight assignment) and thus can be combined. In terms of storage, our pruned nets are light. On a machine with 32-bit parameters the above models are respectively 12MB, 6.9MB, and 4.3MB. Those light models can possibly fit into computer/cellphone memories or even caches (with super-linear efficiency boost).

5 Conclusion

In this paper, we have proposed a neuron level end-to-end pruning approach, which has a LDA-Deconv utility measure that is directly related to the final classification power. It helps design deep models by finding optimal trade-offs between accuracy and efficiency. Rather than evaluate pruning candidates on a local scale (individually or within 1-2 layers), we consider final classification related global dependencies across all layers' neurons/filters. We bring the LDA based conv filter pruning idea to FC structures with many crucial improvements. The structured nature of the approach offers great potential for installation on mobile devices that don't have a powerful GPU. In facial trait classification on LFWA and Adience examples, our approach achieves greater complexity reductions than competing methods (over 98% of VGG-16, 82% of GoogLeNet parameters as well as 83% of VGG-16, 64% of GoogLeNet computations have been saved without obvious accuracy loss).

References

1. Russakovsky, O., Deng, J., Su, H., Krause, J., Satheesh, S., Ma, S., Huang, Z., Karpathy, A., Khosla, A., Bernstein, M., Berg, A.C., Fei-Fei, L.: ImageNet Large Scale Visual Recognition Challenge. *International Journal of Computer Vision (IJCV)* **115**(3) (2015) 211–252
2. LeCun, Y., Denker, J.S., Solla, S.A., Howard, R.E., Jackel, L.D.: Optimal brain damage. In: *NIPs. Volume 2.* (1989) 598–605
3. Han, S., Pool, J., Tran, J., Dally, W.: Learning both weights and connections for efficient neural network. In: *Advances in Neural Information Processing Systems.* (2015) 1135–1143
4. Fisher, R.A.: The use of multiple measurements in taxonomic problems. *Annals of eugenics* **7**(2) (1936) 179–188
5. Tian, Q., Arbel, T., Clark, J.J.: Deep l1-pruned nets for efficient facial gender classification. In: *Computer Vision and Pattern Recognition Workshops (CVPR Workshop on Biometrics), 2017 IEEE Conference on, IEEE* (2017) 512–521
6. Krizhevsky, A., Sutskever, I., Hinton, G.E.: Imagenet classification with deep convolutional neural networks. In: *Advances in neural information processing systems.* (2012) 1097–1105
7. Simonyan, K., Zisserman, A.: Very deep convolutional networks for large-scale image recognition. In: *Proceedings of the International Conference on Learning Representations (ICLR) 2015.* (2015)
8. Szegedy, C., Liu, W., Jia, Y., Sermanet, P., Reed, S., Anguelov, D., Erhan, D., Vanhoucke, V., Rabinovich, A.: Going deeper with convolutions. In: *Proceedings of the IEEE Conference on Computer Vision and Pattern Recognition.* (2015) 1–9
9. Iandola, F.N., Han, S., Moskewicz, M.W., Ashraf, K., Dally, W.J., Keutzer, K.: Squeezenet: Alexnet-level accuracy with 50x fewer parameters and 0.5 mb model size. *arXiv preprint arXiv:1602.07360* (2016)
10. Howard, A.G., Zhu, M., Chen, B., Kalenichenko, D., Wang, W., Weyand, T., Andreetto, M., Adam, H.: Mobilenets: Efficient convolutional neural networks for mobile vision applications. *arXiv preprint arXiv:1704.04861* (2017)
11. Li, H., Kadav, A., Durdanovic, I., Samet, H., Graf, H.P.: Pruning filters for efficient convnets. *arXiv preprint arXiv:1608.08710* (2016)
12. Eidinger, E., Enbar, R., Hassner, T.: Age and gender estimation of unfiltered faces. *IEEE Transactions on Information Forensics and Security* **9**(12) (2014) 2170–2179
13. Turk, M.A., Pentland, A.P.: Face recognition using eigenfaces. In: *Computer Vision and Pattern Recognition, 1991. Proceedings CVPR'91., IEEE Computer Society Conference on, IEEE* (1991) 586–591
14. Belhumeur, P.N., Hespanha, J.P., Kriegman, D.J.: Eigenfaces vs. fisherfaces: Recognition using class specific linear projection. *IEEE Transactions on pattern analysis and machine intelligence* **19**(7) (1997) 711–720
15. Ahonen, T., Hadid, A., Pietikäinen, M.: Face recognition with local binary patterns. In: *European conference on computer vision, Springer* (2004) 469–481
16. Ahonen, T., Hadid, A., Pietikäinen, M.: Face description with local binary patterns: Application to face recognition. *IEEE transactions on pattern analysis and machine intelligence* **28**(12) (2006) 2037–2041
17. Lowe, D.G.: Object recognition from local scale-invariant features. In: *Computer vision, 1999. The proceedings of the seventh IEEE international conference on. Volume 2., Ieee* (1999) 1150–1157
18. Kumar, N., Berg, A.C., Belhumeur, P.N., Nayar, S.K.: Attribute and simile classifiers for face verification. In: *Computer Vision, 2009 IEEE 12th International Conference on, IEEE* (2009) 365–372

19. Štruc, V., Pavešić, N.: Gabor-based kernel partial-least-squares discrimination features for face recognition. *Informatica* **20**(1) (2009) 115–138
20. Golomb, B.A., Lawrence, D.T., Sejnowski, T.J.: Sexnet: A neural network identifies sex from human faces. In: *NIPS*. Volume 1. (1990) 2
21. Poggio, B., Brunelli, R., Poggio, T.: Hyperbf networks for gender classification. (1992)
22. Gutta, S., Wechsler, H.: Gender and ethnic classification of human faces using hybrid classifiers. In: *Neural Networks, 1999. IJCNN'99. International Joint Conference on*. Volume 6., IEEE (1999) 4084–4089
23. Verma, A., Vig, L.: Using convolutional neural networks to discover cognitively validated features for gender classification. In: *Soft Computing and Machine Intelligence (ISCM), 2014 International Conference on*, IEEE (2014) 33–37
24. Levi, G., Hassner, T.: Age and gender classification using convolutional neural networks. In: *Proceedings of the IEEE Conference on Computer Vision and Pattern Recognition Workshops*. (2015) 34–42
25. Mansanet, J., Albiol, A., Paredes, R.: Local deep neural networks for gender recognition. *Pattern Recognition Letters* **70** (2016) 80–86
26. Li, S., Xing, J., Niu, Z., Shan, S., Yan, S.: Shape driven kernel adaptation in convolutional neural network for robust facial traits recognition. In: *Proceedings of the IEEE Conference on Computer Vision and Pattern Recognition*. (2015) 222–230
27. Zhang, N., Paluri, M., Ranzato, M., Darrell, T., Bourdev, L.: Panda: Pose aligned networks for deep attribute modeling. In: *Proceedings of the IEEE Conference on Computer Vision and Pattern Recognition*. (2014) 1637–1644
28. Liu, Z., Luo, P., Wang, X., Tang, X.: Deep learning face attributes in the wild. In: *Proceedings of International Conference on Computer Vision (ICCV)*. (December 2015)
29. He, K., Zhang, X., Ren, S., Sun, J.: Deep residual learning for image recognition. *arXiv preprint arXiv:1512.03385* (2015)
30. Sun, Y., Wang, X., Tang, X.: Deeply learned face representations are sparse, selective, and robust. In: *Proceedings of the IEEE Conference on Computer Vision and Pattern Recognition*. (2015) 2892–2900
31. Pratt, L.Y.: Comparing biases for minimal network construction with back-propagation. Volume 1. Morgan Kaufmann Pub (1989)
32. Hassibi, B., Stork, D.G.: Second order derivatives for network pruning: Optimal brain surgeon. Morgan Kaufmann (1993)
33. Reed, R.: Pruning algorithms—a survey. *IEEE transactions on Neural Networks* **4**(5) (1993) 740–747
34. Han, S., Mao, H., Dally, W.J.: Deep compression: Compressing deep neural network with pruning, trained quantization and huffman coding. *CoRR*, abs/1510.00149 **2** (2015)
35. Srinivas, S., Babu, R.V.: Data-free parameter pruning for deep neural networks. *arXiv preprint arXiv:1507.06149* (2015)
36. Mariet, Z., Sra, S.: Diversity networks. *ICLR* (2016)
37. Jin, X., Yuan, X., Feng, J., Yan, S.: Training skinny deep neural networks with iterative hard thresholding methods. *arXiv preprint arXiv:1607.05423* (2016)
38. Guo, Y., Yao, A., Chen, Y.: Dynamic network surgery for efficient dnns. In: *Advances In Neural Information Processing Systems*. (2016) 1379–1387
39. Hu, H., Peng, R., Tai, Y.W., Tang, C.K.: Network trimming: A data-driven neuron pruning approach towards efficient deep architectures. *arXiv preprint arXiv:1607.03250* (2016)
40. Sze, V., Yang, T.J., Chen, Y.H.: Designing energy-efficient convolutional neural networks using energy-aware pruning. 5687–5695
41. Anwar, S., Hwang, K., Sung, W.: Structured pruning of deep convolutional neural networks. *arXiv preprint arXiv:1512.08571* (2015)

42. Polyak, A., Wolf, L.: Channel-level acceleration of deep face representations. *IEEE Access* **3** (2015) 2163–2175
43. Valiant, L.G.: A quantitative theory of neural computation. *Biological cybernetics* **95**(3) (2006) 205–211
44. Mountcastle, V.B., et al.: Modality and topographic properties of single neurons of cats somatic sensory cortex. *J neurophysiol* **20**(4) (1957) 408–434
45. Mountcastle, V.B.: The columnar organization of the neocortex. *Brain* **120**(4) (1997) 701–722
46. Rinkus, G.J.: A cortical sparse distributed coding model linking mini-and macrocolumn-scale functionality. *Frontiers in neuroanatomy* **4**(17) (2010)
47. Rinkus, G.J.: Sparsity: event recognition via deep hierarchical sparse distributed codes. *Frontiers in computational neuroscience* **8** (2014)
48. Rastegari, M., Ordonez, V., Redmon, J., Farhadi, A.: Xnor-net: Imagenet classification using binary convolutional neural networks. In: *European Conference on Computer Vision*, Springer (2016) 525–542
49. Lin, M., Chen, Q., Yan, S.: Network in network. *ICLR* (2014)
50. He, K., Zhang, X., Ren, S., Sun, J.: Deep residual learning for image recognition. In: *Proceedings of the IEEE conference on computer vision and pattern recognition*. (2016) 770–778
51. Li, Y., Kittler, J., Matas, J.: Effective implementation of linear discriminant analysis for face recognition and verification. In: *Computer Analysis of Images and Patterns*, Springer (1999) 234
52. Bekios-Calfa, J., Buenaposada, J.M., Baumela, L.: Revisiting linear discriminant techniques in gender recognition. *IEEE Transactions on Pattern Analysis and Machine Intelligence* **33**(4) (2011) 858–864
53. Zeiler, M.D., Taylor, G.W., Fergus, R.: Adaptive deconvolutional networks for mid and high level feature learning. In: *2011 International Conference on Computer Vision*, IEEE (2011) 2018–2025
54. Zeiler, M.D., Fergus, R.: Visualizing and understanding convolutional networks. In: *European Conference on Computer Vision*, Springer (2014) 818–833
55. Long, J., Shelhamer, E., Darrell, T.: Fully convolutional networks for semantic segmentation. In: *Proceedings of the IEEE Conference on Computer Vision and Pattern Recognition*. (2015) 3431–3440
56. Hebb, D.O.: *The organization of behavior: A neuropsychological theory*. Psychology Press (2005)
57. Rothe, R., Timofte, R., Gool, L.V.: Deep expectation of real and apparent age from a single image without facial landmarks. *International Journal of Computer Vision (IJCV)* (July 2016)
58. Huang, G.B., Ramesh, M., Berg, T., Learned-Miller, E.: Labeled faces in the wild: A database for studying face recognition in unconstrained environments. Technical Report 07-49, University of Massachusetts, Amherst (October 2007)